Geomicrobiology Journal

ISSN: 0149-0451 (Print) 1521-0529 (Online) Journal homepage: https://www.tandfonline.com/loi/ugmb20

Microbial Community Structure and Metabolic Potential of the Hyporheic Zone of a Large Mid-Stream Channel Bar

Joshua D. Sackett, Christopher L. Shope, James C. Bruckner, Journét Wallace, Clay A. Cooper & Duane P. Moser

To cite this article: Joshua D. Sackett, Christopher L. Shope, James C. Bruckner, Journét Wallace, Clay A. Cooper & Duane P. Moser (2019): Microbial Community Structure and Metabolic Potential of the Hyporheic Zone of a Large Mid-Stream Channel Bar, Geomicrobiology Journal, DOI: 10.1080/01490451.2019.1621964

To link to this article: https://doi.org/10.1080/01490451.2019.1621964

GEOMICROBIOLOGY JOURNAL
https://doi.org/10.1080/01490451.2019.1621964

Taylor & Francis
Taylor & Francis Group

Microbial Community Structure and Metabolic Potential of the Hyporheic Zone of a Large Mid-Stream Channel Bar

Joshua D. Sackett[a,b,c], Christopher L. Shope[d], James C. Bruckner[a], Journét Wallace[a,c], Clay A. Cooper[e], and Duane P. Moser[a,b]

[a]Division of Earth and Ecosystem Sciences, Desert Research Institute, Las Vegas, NV, USA; [b]Division of Hydrologic Sciences, Desert Research Institute, Las Vegas, NV, USA; [c]School of Life Sciences, University of Nevada, Las Vegas, NV, USA; [d]Division of Water Quality, Utah Department of Environmental Quality, Salt Lake City, UT, USA; [e]Division of Hydrologic Sciences, Desert Research Institute, Reno, NV, USA

ABSTRACT

To develop a greater understanding of hyporheic zone microbial biogeochemistry, we sampled pore fluids from a piezometer array associated with the McCarran Ranch channel bar (MRCB); a partially submerged cobble island in the Truckee River, NV, USA. Flowing surface water and pumped pore fluids were characterized by prokaryotic community structure, metabolic potential, and aqueous physicochemistry. Concentrations of potential respiratory electron acceptors were highest in surface water and riverbed porewater and sequentially depleted in porewaters along the inferred flowpath (O_2, then NO_3^-, then SO_4^{2-}). Correspondingly, cultivable nitrate reducers/denitrifiers were most abundant in surface water and riverbed porewater, despite oxic conditions. Cultivable sulfate reducers were overall most abundant in surface water. Prokaryotic community reconstruction from 16S rRNA gene sequences indicates that the surface water community was less diverse than that of porewater and supports a shift in metabolic strategy, from aerobic heterotrophy in surface water (e.g., Comamonadaceae and Sporichthyaceae) to chemolithotrophy and anaerobic metabolisms (e.g., *Hydrogenophaga* spp., *Ferribacterium* spp., *Methanobacterium* spp.) along the hyporheic flow path. These data indicate that prokaryotic communities within the MRCB are phylogenetically and metabolically diverse and contribute to biogeochemical cycling in this common yet relatively understudied habitat.

ARTICLE HISTORY
Received 5 February 2019
Accepted 16 May 2019

KEYWORDS
Anaerobic metabolism; aqueous biogeochemistry; denitrification; prokaryotic diversity; Truckee River

Introduction

Hyporheic zones have been classified as 'biogeochemical hotspots' (Craig et al. 2010; McClain et al. 2003; Stegen et al. 2018) due to the influx and mixing of dissolved organic carbon (DOC) compounds, nutrients, and electron acceptors from surface water with groundwater (Findlay 1995; Findlay et al. 1993, 2003; Hendricks 1993). This influx of DOC, nutrients, and electron acceptors stimulates microbial activity, which is estimated to be responsible for 75–90% of total river ecosystem respiration (Naegeli and Uehlinger 1997). Multiple studies have demonstrated that hyporheic zones serve as ecologically important sinks for organic carbon, oxygen, and nitrogen (primarily nitrate) (Febria et al. 2010; Findlay 1995; Findlay et al. 1993, 2003; Goldman et al. 2017; Hendricks 1993; Hou et al. 2017; Moser et al. 2003; Naegeli and Uehlinger 1997; Stegen et al. 2018). Furthermore, Stegen et al. (2018) demonstrated that shifts in DOC composition from terrestrially derived lignin-like DOC in surface water to labile but low concentration DOC in groundwater exert strong deterministic selection pressures that differentiate microbial communities in surface water, the hyporheic zone, and groundwater.

Microbial nitrate reduction/denitrification has been documented in a number of hyporheic zone environments (Hill and Lymburner 1998; Morrice et al. 2000), including overall oxygenated systems (Duff and Triska 1990; Holmes et al. 1996; Lefebvre et al. 2004; Moser et al. 2003), where it likely occurs in anoxic microniches. Likewise, sulfate-reducing microorganisms have been cultured from hyporheic fluids (Moser et al. 2003), suggesting that microorganisms in the hyporheic zone have the potential for sulfate reduction. Similar to what has been observed for fully submerged and parafluvial hyporheic zones (Duff and Triska 1990; Hill and Lymburner 1998; Holmes et al. 1996; Lefebvre et al. 2004; Morrice et al. 2000; Moser et al. 2003), Zarnetske et al. (2011) have measured the rapid utilization of dissolved oxygen and dissolved organic carbon, followed by strong induction of denitrification (anaerobic metabolism) in a gravel bar hyporheic zone. Reactive transport models have shown that hyporheic zones, particularly those dominated by partially submerged morphological structures such as channel bars, have a higher capacity for anaerobic respiration (nitrate reduction, denitrification, sulfate reduction) compared to fully submerged geomorphic structures due to increased water residence times (Trauth et al. 2015). These

CONTACT Duane P. Moser duane.moser@dri.edu Division of Hydrologic Sciences, Desert Research Institute, 755 E Flamingo Rd., Las Vegas 89119, NV, USA.

Supplemental data for this article can be accessed here.

observations highlight the importance of partially submerged riverine features for hyporheic interactions and nutrient exchange (Shope et al. 2012) and predicted higher capacity for denitrification (Trauth et al. 2015) compared to fully submerged features. Thus, hyporheic exchange and microbial activity in partially submerged channel bars may be an ecologically important sink for natural and anthropogenic sources of nitrogen (Ock et al. 2015) and sulfate.

More recently, 16S rRNA gene surveys have allowed for comprehensive characterization of hyporheic zone microbial communities (Goldman et al. 2017; Hou et al. 2017; Stegen et al. 2018). For example, Goldman et al. (2017) showed that inundation dynamics drive bacterial, archaeal, and fungal community structures and aerobic respiration rates in parafluvial hyporheic zone sediments. Hou et al. (2017) demonstrated that microbial density and community structure in hyporheic zone sediments are affected by permeability, with coarse-grained material having higher biomass and microbial activity than fine-grained material. Stegen et al. (2018) found that differences in microbial community structure between river water and hyporheic zone communities were associated with shifts in DOC composition (lignin-like compounds in river water and amino sugar compounds in the hyporheic zone).

Despite much progress in our understanding of hyporheic zones of submerged features (e.g., riverbeds) and parafluvial features (e.g., river banks), less attention has been given to partially submerged fluvial features, such as gravel bars and fluvial islands, given their abundance in rivers (Osterkamp 1998). Stream water enters the hyporheic zone of fluvial islands through advective flow where residence time and flow paths are strongly influenced by hydraulic gradients, stream morphology, and river stage (Dent et al. 2007; Findlay 1995; Francis et al. 2010; Schmidt et al. 2012; Shope et al. 2012; Trauth et al. 2015). Upon infiltration of river water into the hyporheic zone, the influx of electron acceptors (O_2, NO_3^-, SO_4^{2-}) drives the oxidation of both groundwater-derived and stream water-derived DOC (Stegen et al. 2018). Once oxygen concentrations have been depleted, nitrate reduction and denitrification, followed by sulfate reduction, are the preferred alternative energy pathways for a wide variety of microorganisms when dissolved oxygen concentrations are limiting but nitrate and/or sulfate remain available.

The objective of this study was to obtain a robust understanding of microbial community structure and metabolic potential from the surface and porewater fluids collected along a transect through the McCarran Ranch channel bar (MRCB), a partially submerged fluvial geomorphic feature composed of well-sorted large cobble in the Truckee River, Nevada, USA. Utilizing fluids pumped from a previously installed hydrologic piezometer array (Shope et al. 2012), we characterized the bacterial and archaeal community structure, metabolic potential through cultivation studies, and aqueous chemistries of flowing river surface water and porewater in parallel to better understand microbial biogeochemical transformations in the MRCB. Our study highlights the ecological importance of hyporheic zones from partially submerged fluvial islands in nutrient and elemental cycling and a potential role of these common, yet relatively understudied features in the natural attenuation of anthropogenic contaminants, such as nitrate.

Materials and methods

Site description and hydraulic properties

The McCarran Ranch channel bar (MRCB) is a long-lived geomorphic feature of the Truckee River located 27 km east of Reno, Nevada (39°32′49.05 N 119°33′30.01 W, Figure 1) and 16 km downstream of the Truckee Meadows Water Reclamation Facility (TMWRF), which discharges 1.5×10^8 L/d of treated wastewater (Mortensen et al. 2007). At the time of sampling, TMWRF discharge contributed approximately 70% to Truckee River base flow (Mortensen et al. 2007; USGS 2017). The channel bar (60 × 198 m) is oriented roughly southwest/northeast with the long axis running parallel to the flow of the river and exhibits a 1.46 m surface elevation drop over its length. The bar is separated from the shoreline by flowing river channels of about 30 m width on both sides. Under base flow conditions, the highest MRCB surface is approximately 1.2 m above the river stage and the southeast river channel is approximately 0.2 m higher than the northwest river channel (Shope et al. 2012). The bar was reworked during flooding in the late 1990s and is composed of coarse, well-sorted stream cobble, with varying amounts of silt occupying relatively large pores between the cobble and little sand. The lateral edges of the MRCB are occupied by dense stands of Fremont Cottonwood (*Populus fremontii*), willow (*Salix boothi*), and Mountain Alder (*Alnus incana*).

In the early 2000s, an expansive piezometer array was installed throughout the MRCB and adjacent river channel for a study of fluid flow dynamics through the channel bar. The piezometers consisted of 2.1 cm schedule 40 PVC pipe, mechanically inserted into the coarse substrate to depths ranging from 1.11–1.78 m below ground surface and screened over the bottom 2–5 cm. Work using temperature loggers, pressure transducers, and stage recorders from this piezometer network within and around the channel bar revealed a complex mixing regime between groundwater and river water (Shope et al. 2012). Groundwater mounding throughout the MRCB is variable and largely dependent on river stage, although, under base flow conditions, groundwater mounds exist ~60 m downstream of the leading edge of the MRCB and 5–10 m upstream of the tail end of the MRCB (Shope et al. 2012). However, transient groundwater mounds and depressions develop seasonally and following precipitation events. Specifically, on 11 September 2007 (six days prior to sample collection), lateral water flow (southward) from the northwestern river channel to piezometer IW27 (Figure 1), due to a transient hydraulic gradient, and a groundwater depression near the leading edge of MRCB was observed (Shope et al. 2012). Hydraulic conductivity estimates of the bar from falling-head slug tests ranged from 2.03×10^{-4} m/s to 3.29×10^{-7} m/s (Shope et al. 2012),

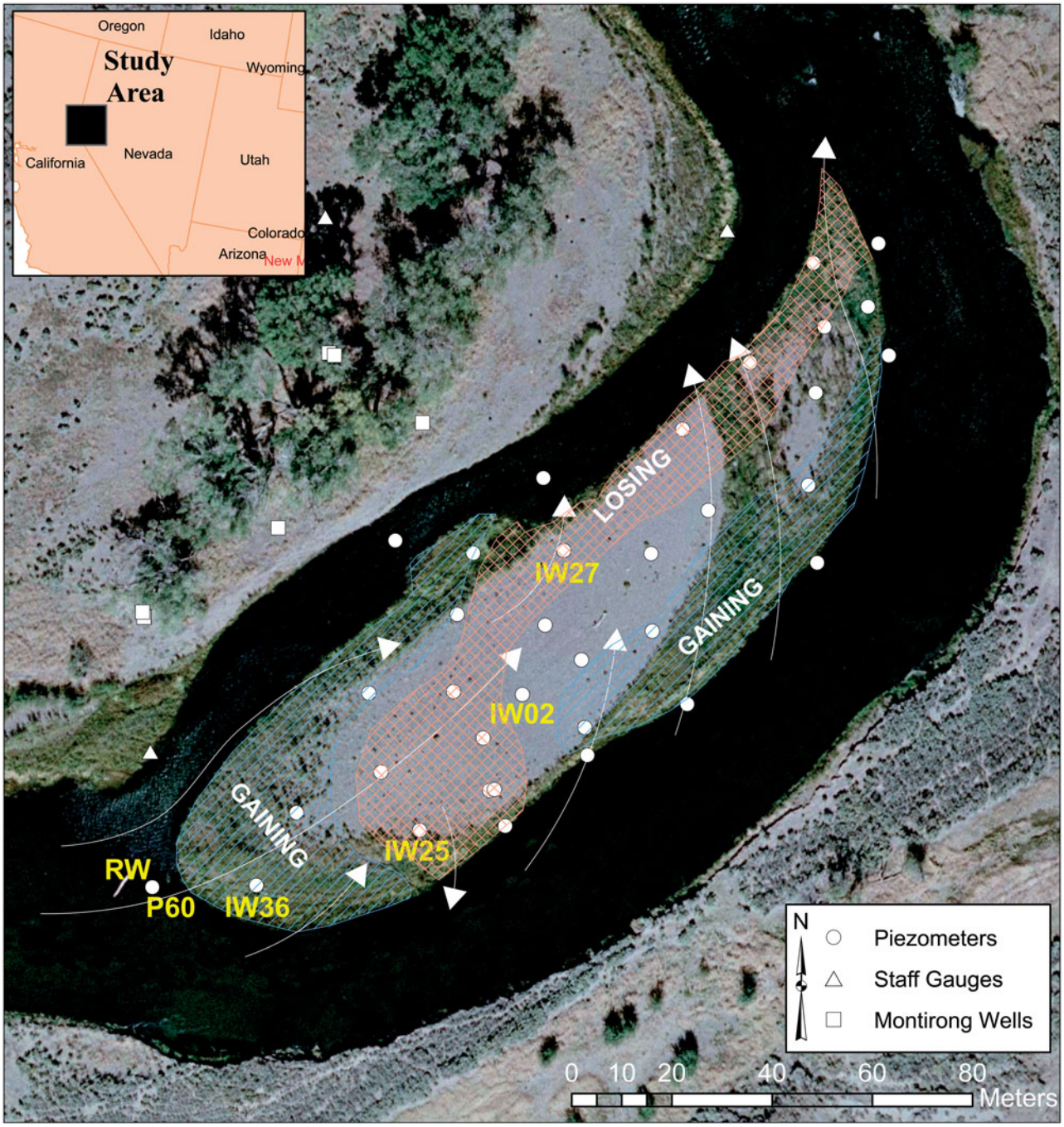

Figure 1. Study site. The McCarran Ranch channel bar, a fluvial geomorphic feature in the Truckee River, is located 29 km east of Reno, NV. Sample locations and sample names are noted. Generalized hyporheic flow paths are shown as white arrows and regions where the channel bar is gaining (infiltration) and losing (exfiltration) water from hyporheic flow are indicated by blue and red hatch polygons, respectively (adapted from Shope et al. 2012). Dense stands of Fremont Cottonwood (*Populus fremontii*), willow (*Salix boothi*), and Mountain Alder (*Alnus incana*) are present along the edges of the channel bar.

suggesting that water residence times through the MRCB could be highly spatially variable.

Sample collection and physical measurements

Samples and physical measurements were obtained from water pumped from river surface water (RW) and piezometers (P60, IW36, IW25, IW02, and IW27) with a portable Masterflex E/S peristaltic pump (Cole-Parmer, Vernon Hills, IL) and autoclaved LS-15 platinum-cured silicone tubing (Cole-Parmer, Vernon Hills, IL) on 17 September 2007. With the exception of P60, all piezometers were located within the MRCB. P60 was positioned within a riffle ~10 m upstream of the leading edge of the MRCB. Prior to sample collection, 1 L of water was pumped from each of the piezometers and discarded to minimize the impact of stagnant water within the piezometer. Dissolved oxygen, temperature, and conductivity measurements were taken with a YSI 6600 sonde and multiparameter meter (YSI, Inc., Yellow Springs, OH) fitted with a flow cell. Turbidity measurements were obtained using a LaMotte 2020 meter (LaMotte, Chesterton,

MD). Water samples for chemical analysis were passed through 0.22 µm nylon filters (Pall, Port Washington, NY), collected in triple-rinsed 500 mL HDPE plastic bottles (Nalgene) and stored on ice or refrigerated until analyzed (within 2 days). Microbial biomass for DNA analysis was concentrated on 0.22 µm Supor polyethersulfone membrane filters (Pall) from 500–750 mL of water per sample (60 mL for RW due to the abundance of suspended particulate matter which clogged the filter) and frozen onsite using dry ice. Samples for microbial cultivations were collected in sterile 50 mL polypropylene conical centrifuge tubes, placed immediately on ice, and used for inoculations in the laboratory within 24 h. Samples for microbial direct counts were taken in the same manner but preserved with 2.5% (v/v) glutaraldehyde.

Chemical analysis of porewater and river water

Alkalinity measurements were performed in the field by titrating to pH 4.5 using the reagents and autotitrator from a Hach Alkalinity kit (LHC20637-00, Hach, Loveland, CO) and portable pH meter (LaMotte, Chestertown, MD). All other chemical analyses were performed at the Desert Research Institute Water Laboratory (Reno, NV) according to EPA procedures (Greenberg et al. 1992; USEPA 1979, 1993). Nitrate, nitrite, ammonium, and phosphate were analyzed using automated colorimetric analyzers (Alpkem RFA 300 and Technicon Automated Colorimetric Analyzer) and EPA methods SM 4500-NO3 F, SM 4500-NH4 F, and SM 4500-P E. Dissolved organic carbon (DOC) was measured with an Astro 2001 Carbon Analyzer using heated persulfate oxidation, followed by IR measurement of the non-purgeable organics (EPA method SM 5310 C). Sulfate was measured according to EPA method 300 by ion chromatography (Dionex Model ICS 2000, Dionex, Sunnyvale, CA). Soluble iron and manganese were measured with a Thermo Elemental SOLAAR M5 Atomic Absorption Spectrometer according to EPA method (SM 3111B, Thermo, Carlbad, CA).

Cultivation of microorganisms

Densities of cultivable microbial cells of key physiotypes were estimated using the most probable number (MPN) technique (Woomer 1994). Incubations were performed without agitation at room temperature (~22 °C) to approximate environmental conditions and results were recorded 1 week after inoculation. Except when otherwise noted, cultures were scored as positive for growth based upon visible turbidity. Aerobic heterotrophs were enumerated using R2B liquid medium (Reasoner and Geldreich 1985) diluted to extinction (serial 10-fold) in duplicate slip-cap culture tubes (16 mm, borosilicate). Anaerobic cultivations (for nitrate-, sulfate-, and iron-reducing bacteria) were performed using the Hungate technique (Balch et al. 1979; Miller and Wolin 1974) in 18 mm Balch tubes, crimp sealed with blue butyl rubber stoppers (Bellco Glass) with an $H_2/CO_2/N_2$ headspace (5%/20%/75%). Anaerobic media were pre-reduced using 0.025% (w/v) cysteine-HCl, and anaerobic status was confirmed by the addition of the redox indicator resazurin (1 µg/mL). Nitrate-reducing microorganisms were cultivated in R2B broth plus 0.05% (w/v) KNO_3 and assessed for growth by visual turbidity, nitrate reduction to nitrite with Nitrate Reagents A, B, and C (Hardy Diagnostics, Santa Maria, CA), and gas production (presumably N_2) as evidenced by the accumulation of gas inside an inverted Durham tube (Greenberg et al. 1992). Iron-reducing microorganisms were cultivated in M1 medium (Myers and Nealson 1988) with sodium lactate, acetate, and formate (5 mM each) added as electron donors, and Fe(III)-nitrilotriacetate (10 mM) as an electron acceptor (Kostka and Nealson 1998). A change from turbid orange to clear with a dark brown precipitate (magnetite) was considered indicative of iron-reducing microorganisms. Sulfate-reducing microorganisms were cultivated in Postgate Medium B (Postgate 1984) and scored based on the formation of turbidity and black precipitates.

Microscopy

Direct microbial cell counts were performed as described previously (Moser and Nealson 1996; Porter and Feig 1980). Briefly, 1.0 mL aliquots of glutaraldehyde-fixed cells were stained with 0.03% (w/v) 4′-6-diamidino-2-phenylindole (Sigma-Aldrich, Darmstadt, Germany), concentrated onto 25 mm, 0.22 µm black polycarbonate membrane filters (GE Osmonics, Inc., Minnetonka, MN), and washed with two volumes of deionized H_2O. Fluorescing cells were counted from >30 fields on randomized slides (to eliminate user bias) using a Zeiss Axioscope microscope (Zeiss, Oberkochen, Germany) equipped with a DAPI-FITC filter. Original cell densities were estimated by back calculation.

DNA extraction, library preparation, and 16S rRNA gene sequencing

Total genomic DNA was isolated from one 0.22 µm polyethersulfone filter per sample location with the MoBio PowerSoil DNA Isolation Kits (MoBio, Carlsbad, CA) according to the manufacturer's instructions, with the addition of a freeze-thaw step prior to bead-beating (30 min at −80 °C, 10 min at 65 °C). Library preparation and Illumina sequencing were performed at Molecular Research LP (MR DNA, Shallowater, TX). Library preparation was carried out through PCR using modified primer sequences targeting the V4 hypervariable region of the 16S rRNA gene found in Prokaryotes (F515 [5′-GTGYCAGCMGCCGC GGTAA-3′] (Parada et al. 2016) and 806 R [5′-GGACTACHVGGGTWTCTAAT-3′] (Caporaso et al. 2011)), with 8-nucleotide, sample-specific barcodes on the forward primer. PCR products from all samples were quantified, normalized, and pooled. This PCR product pool was then purified with Agencourt AMPure XP beads (Beckman Coulter, Inc., Brea, CA) and used to generate a sequencing library according to the Illumina TruSeq DNA PCR-Free library preparation kit protocol (Illumina, San Diego, CA). The final sequencing library was sequenced in one

Table 1. Physical and chemical characteristics of water samples.

	[a]RW	[b]P60	IW36	IW25	IW02	IW27
Physical measurements						
Temp (°C)	18.7	19.03	21.39	20.37	23.02	22.9
Turbidity (NTU)	3.43	3.15	3.58	2.72	2.48	2.73
Conductivity (mS/cm)	0.258	0.268	0.280	0.270	0.283	0.318
pH	8.18	7.60	7.00	6.65	6.94	6.84
dO_2 (mg/L)	9.58	2.69	2.35	1.06	0.96	0.87
dO_2 (% saturation)	102.3	35.9	27.3	11.8	11.2	10.1
Carbon/phosphorus (mg/L)						
Alkalinity as $CaCO_3^-$	72	78	86	84	88	112
DOC	2.9	1.7	2.1	2.6	2.0	1.8
P as O-PO_4^-	0.024	0.063	0.036	0.094	0.044	0.071
Anaerobic electron acceptors (mg/L)						
N as NO_3^-	0.015	0.015	0.006	0.003	0.004	0.003
N as NO_2^-	0.001	<0.001	<0.001	0.001	0.002	0.002
SO_4^{2-}	23.6	22.9	17.4	13.6	17.1	12.7
Electron donors (mg/L)						
[c]Fe^{2+}	0.03	0.16	2.77	1.88	2.63	0.53
[d]Mn^{2+}	0.02	0.20	0.65	0.78	0.71	0.06
N as NH_3	0.014	0.053	0.311	0.122	0.381	0.020

aSurface water sample. [b]River porewater/hyporheic zone sample. [c]Soluble iron (field filtered) assumed to be mostly in the ferrous (Fe^{2+}) state. [d]Soluble manganese (field filtered) assumed to be mostly in the manganous (Mn^{2+}) state.

Illumina MiSeq instrument run using the 2x300 MiSeq Reagent Kit v2 according to the manufacturer's guidelines (Illumina, San Diego, CA). The raw, demultiplexed 16S rRNA gene sequence libraries were deposited in the European Nucleotide Archive under project accession number PRJEB25995.

16S rRNA gene sequence libraries analysis

Raw 16S rRNA gene sequence libraries were analyzed with QIIME 1.9.1 (Caporaso, Kuczynski, et al. 2010). In total, 396,171 paired-end reads were generated (Table S1). Because read length (300 base pairs [bp]) was longer than predicted amplicon length (~291 bp), forward and reverse reads were trimmed to 250 bp with the truncate_fasta_qual_files.py command. The resulting trimmed paired-end reads were merged according to the fastq-join method (Aronesty 2011) using default parameters. Merged reads containing ambiguous ('N' characters) and low-quality base calls (Phred score <30) were removed. Chimeric sequences were identified with the usearch61 algorithm (Edgar 2010) and removed. Operational taxonomic units (OTUs) were generated from the 207,068 high-quality nonchimeric sequences, based on 97% sequence similarity, and taxonomy assignments made with a subsampled open-reference OTU-picking strategy using usearch61 and uclust (Edgar 2010) against the SILVA_128 curated database (Pruesse et al. 2007; Quast et al. 2013; Yilmaz et al. 2014). OTUs supported by less than 0.005% of all sequences (10 sequences per OTU) were removed. A phylogenetic neighbor-joining tree (Price et al. 2010), based on PyNAST-aligned OTU sequences (Caporaso, Bittinger, et al. 2010), was generated and used for alpha and beta diversity metrics. Lastly, the OTU table was rarefied to a depth of 10,000 sequences per sample to account for differences in sequencing depth. Alpha diversity metrics (observed OTU richness, Chao1 estimated richness, Faith's Phylogenetic Diversity index, and Shannon's index) and pairwise UniFrac (Lozupone et al. 2011) distances between samples were calculated from 100 rarefied OTU tables.

Data analysis

Figures were generated and subsequent analyses were conducted in R (R Core Team 2014) with the vegan v. 2.2-1 (Oksanen et al. 2015) and ape v. 3.2 (Paradis et al. 2004) packages. Clustering of prokaryotic communities was evaluated by constructing a dendrogram based on unweighted pair group method with arithmetic mean (UPGMA)-clustering of abundance-weighted and -unweighted UniFrac distances. Node support values were calculated from 100 rarefied OTU tables of 10,000 sequences per sample. Principal coordinate analysis ordinations were constructed for abundance-weighted and -unweighted UniFrac distances. Chemistry data (with the exception of dissolved oxygen percent saturation values) were normalized by z-score transformation and pairwise Euclidean distances between samples were calculated. Individual chemistry values below the limit of detection were set to zero to allow for calculation of z-scores. A principal component analysis ordination was generated from these pairwise Euclidean distances to identify similarities of chemical profiles between samples.

Results

Field measurements and water chemistry

Physical and chemical characteristics of water samples are shown in Table 1. Surface river water (RW) upstream of the piezometer network was characterized by the highest pH, dissolved oxygen (DO) concentration, dissolved organic carbon (DOC) concentration, and highest concentrations of two potential anaerobic electron acceptors (NO_3^- and SO_4^{2-}) compared to all piezometer samples. DO ranged from fully saturated in flowing surface water and 36% of saturation in the riverbed sample (P60) to a measured low value of ~10% of saturation in the most down-gradient sample (IW27). As with DO, overall, concentrations of NO_3^- and SO_4^{2-} generally declined along the inferred hyporheic flow path (Table 1, Figure 2); whereas, the concentration of dissolved inorganic carbon (DIC), another

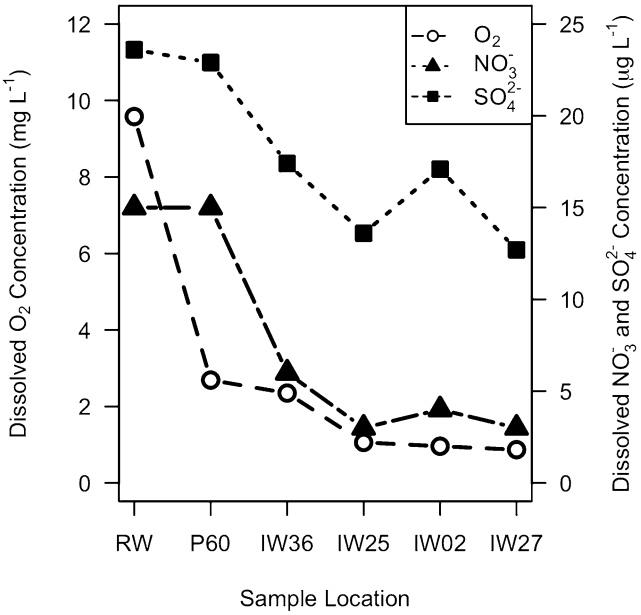

Figure 2. Major electron acceptor concentrations. Changes in concentrations of major electron acceptors (O_2, NO_3^-, and SO_4^{2-}) along the inferred hyporheic flow path (from left to right in the diagram) from single measurements. Dissolved O_2 concentrations (open circles with a dashed line) are plotted against the left axis in mg/L. Dissolved NO_3^- and SO_4^{2-} concentrations (triangles with a dot-dashed line and squares with a dotted line, respectively) are plotted against the right axis in µg/L.

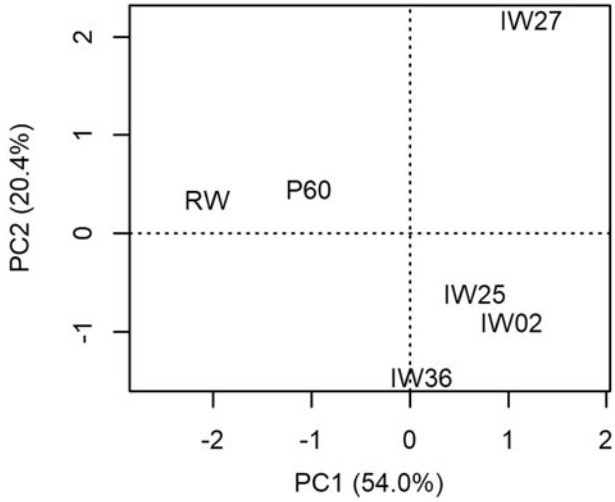

Figure 3. Chemistry PCA. Principal component analysis ordination of pairwise Euclidean distances between samples of z-score-transformed chemistry data (Table 1). Collectively, PC1 and PC2 account for 74.4% of the variation among these six chemistry profiles.

potential electron acceptor, increased. Conversely, the concentrations of alkalinity, orthophosphate, and physiological electron donors (Fe^{2+}, Mn^{2+}, and NH_3) were lowest in RW; with the concentration of electron donors generally increasing along the inferred flow path (Table 1). Considering only dissolved organic carbon concentrations, C:N:P molar ratios were approximately 85:3:1 for RW, 19:2:1 for P60, 41:19:1 for IW36, 19:3:1 for IW25, 32:19:1 for IW02, and 18:1:1 for IW27.

The riverbed porewater sample (P60), collected from ~48 cm below the riverbed, had similar physicochemical characteristics to RW (Figure 3). Despite their close physical proximity, pH, DO, and DOC were lower and the concentrations of electron donors were higher in P60 relative to RW. With the exception of IW27 at the downstream end of the channel bar, porewater chemistry profiles for channel bar samples were similar (Figure 3). The chemical profile of IW27 porewater was characterized by higher alkalinity and lower DO, SO_4^{2-}, Fe^{2+}, Mn^{2+}, and NH_3 compared to all other samples within the channel bar.

Enumeration of microbial physiotypes

Cell density was highest in RW as compared to the piezometer samples (2.8×10^6 cells/mL, Table 2). Cell densities from piezometer porewater samples ranged from 2.8×10^5 to 8.2×10^5 cells/mL and displayed no apparent pattern throughout the MRCB. The concentration of cultivable aerobic heterotrophs was highest in RW and P60, decreased to 2.3×10^2 cells/mL at IW25, and increased by an order of magnitude at IW02 and IW27. The concentrations of cultivable microorganisms capable of dissimilatory nitrate reduction and gas production from denitrification followed a pattern similar to that of cultivable aerobic heterotrophs, with the highest concentrations being found in RW and P60. Cultivable denitrifiers were found in low concentrations or were undetected throughout MRCB porewater samples. Cultivable sulfate reducers were detected in all samples, with the highest concentrations in IW25 and RW. Cultivable Fe^{3+} reducers were only detected in RW.

Prokaryotic community structure

In total, 3108 operational taxonomic units (OTUs) were identified from the 150,101 quality- and abundance-filtered sequences analyzed in the 16S rRNA gene libraries (Appendix S1, Sheet 1). The microbial community of RW was the least diverse of all samples (Student's *t*-test, $p < 0.001$ for all metrics, Table S2). OTU richness, Chao1 estimated richness, and Faith's phylogenetic diversity (PD) estimates for P60 were twice as high as RW. Alpha diversity metrics remained relatively constant among all porewater samples (P60, IW36, IW25, IW02, and IW27). However, hierarchical clustering of abundance-weighted UniFrac distances, a quantitative measure of phylogenetic similarity between pairs of samples, indicated that the microbial community structure of RW was most similar to the microbial community structures of P60 and IW25 despite having significantly lower alpha diversity (Figure S1). Likewise, IW27, IW02, and IW36 formed their own clade in the cluster diagram, indicative of similar microbial community structures among these samples.

The RW sample was dominated by Betaproteobacteria, Actinobacteria, and Bacteroidetes (Figure 4; Appendix S1, Sheet 3). The most abundant OTUs detected in RW were an OTU in the Comamonadaceae family of Betaproteobacteria (OTU 900, 9.3% relative abundance), an OTU in the *Pseudarcicella* genus of Bacteroidetes (OTU 613, 7.8%), two OTUs in the hgcl clade of the Sporichthyaceae family of Actinobacteria (OTUs 803 and 916, 4.7% and 3.8% relative

Table 2. Cell numbers (cells/mL) from raw water samples (direct microscopic counts) and for microbial physiotypes determined from *in vitro* cultivation.

	RW	P60	IW36	IW25	IW02	IW27
Direct counts (DAPI staining)	2.5×10^6	8.1×10^5	5.2×10^5	8.2×10^5	2.8×10^5	3.2×10^5
[a]Aerobic heterotrophs	7.0×10^6	2.3×10^5	6.1×10^2	2.3×10^2	5.9×10^3	2.3×10^3
[a]Nitrate reducers						
[b]Growth	5.9×10^3	2.3×10^4	2.3×10^2	4.6×10^0	2.3×10^3	2.3×10^1
[c]Nitrate reduction	5.9×10^3	1.3×10^3	2.3×10^2	n.d.	2.3×10^2	2.3×10^1
[d]Gas production	6.0×10^0	6.1×10^2	6.1×10^1	n.d.	6.0×10^0	2.3×10^1
[a]Iron reducers	6.1×10^1	n.d.	n.d.	n.d.	n.d.	n.d.
[a]Sulfate reducers	2.3×10^3	6.1×10^1	6.1×10^1	5.9×10^3	6.1×10^1	6.1×10^2

n.d.: not detected. [a]Confidence factor: 6.61. Divide and multiply population estimate by confidence factor to establish 95% confidence interval. [b]Based upon visible turbidity in culture tube. [c]Confirmed with Hardy Diagnostics (Santa Maria, CA) Nitrate Reagents A, B, and C. [d]Inferred from gas accumulation in an inverted Durham tube.

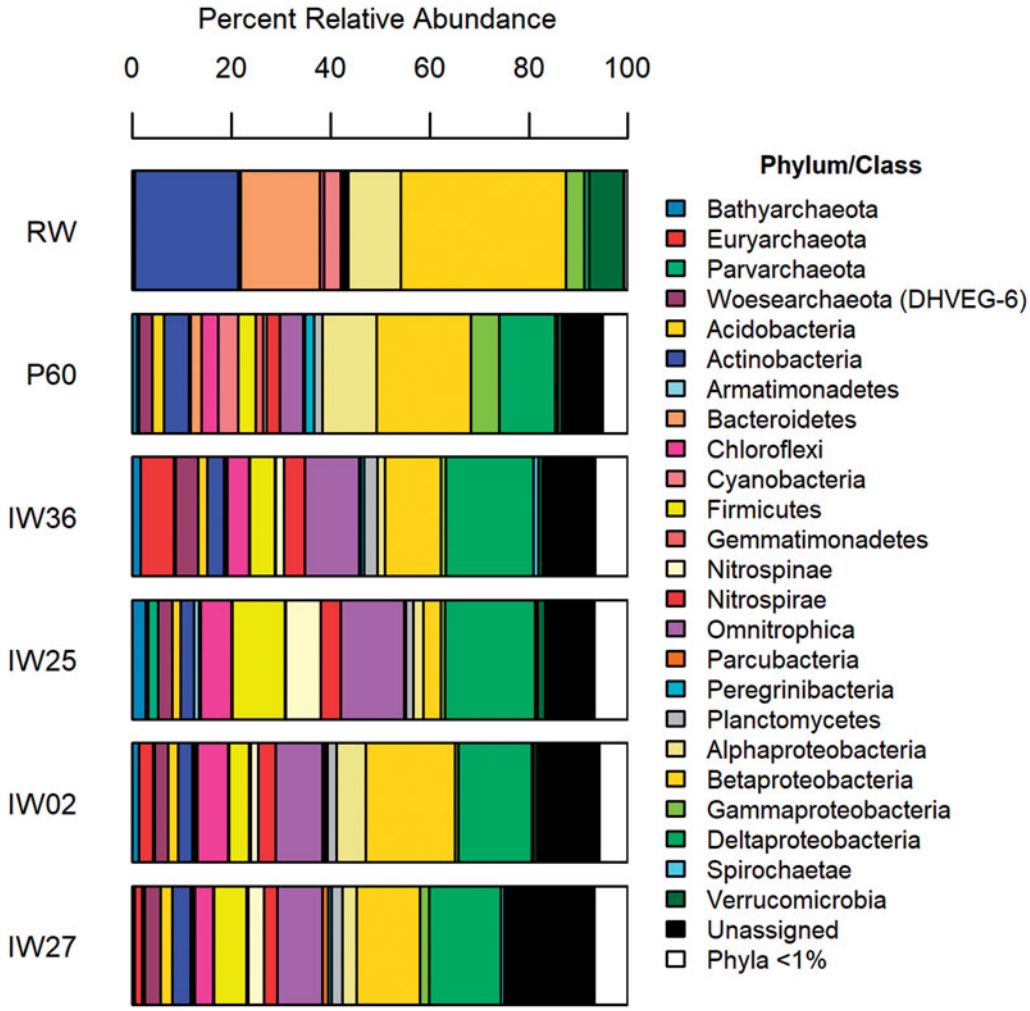

Figure 4. Prokaryotic community composition. Phylum-level taxonomic bar chart for prokaryotic communities from Truckee River and McCarran Ranch channel bar surface and porewater samples. The Proteobacteria have been subdivided into classes. Only prokaryotic phyla/classes with abundances ≥1% are shown. Phyla/classes present in <1% are included collectively as 'Phyla <1%.'

abundance), and an OTU identified as the Betaproteobacterium *Acidovorax facilis* (OTU 889, 3.5%) (Table S3). The riverbed porewater sample (P60) was dominated by Betaproteobacteria, Deltaproteobacteria, Alphaproteobacteria, and Unassigned taxa. The most abundant OTUs in P60 were an OTU in the *Dechloromonas* genus of Betaproteobacteria (OTU 269, 3.7%), an OTU in the *Rhodobacter* genus of Alphaproteobacteria (OTU 574, 2.8%), an OTU in the *Rhodococcus* genus of Actinobacteria (OTU 619, 2.3%), an OTU in the *Sideroxydans* genus of Betaproteobacteria (OTU 897, 1.8%), and an OTU in the *Ruminiclostridium* genus of Firmicutes (OTU 2555, 1.4%). These five OTUs were comparatively rare (<0.2%) in all other samples.

With the exception of IW25, microbial communities from porewater samples within the channel bar were similar (Figure 4; Figure S1). In general, these communities were dominated by Deltaproteobacteria, Betaproteobacteria,

Omnitrophica (OP3), and Unassigned taxa. The most abundant OTUs within the channel bar were an OTU in the *Hydrogenophaga* genus of Betaproteobacteria (OTU 809, $\bar{x}$ = 7.0%), an OTUs in the *Methanobacterium* genus of Euryarchaeota (OTU 538, $\bar{x}$ = 2.4%), an OTU in the *Ferribacterium* genus of Betaproteobacteria (OTU 276, $\bar{x}$ = 1.8%), an OTU in the Peptococcaceae family of Firmicutes (OTU 624, $\bar{x}$ = 1.4%), and an OTU in the *Candidatus* Omnitrophus genus of Omnitrophica (OTU 220, $\bar{x}$ = 1.2%) (Table S3).

The IW25 microbial community, which formed a clade with P60 and RW (Figure S1), was dominated by Deltaproteobacteria, Omnitrophica, Firmicutes, and Unassigned taxa (Figure 4; Appendix S1, Sheet 3). The most abundant OTUs were an OTU in the Belgica2005-10-ZG-3 class of Nitrospinae (OTU 2229, 2.4%), an unclassified OTU belonging to Omnitrophica (OTU 1345, 1.7%), an OTU in the Halanaerobiales order of Firmicutes (OTU 1855, 1.4%), an unclassified OTU in the *Parvarchaeota phylum* (OTU 2051, 1.4%), and an OTU in the *Hydrogenophaga* genus of Betaproteobacteria (OTU 809, 1.4%), which was also the most abundant OTU among all other channel bar porewater communities (Table S3).

Discussion

Physical and chemical parameters

Measured DOC, nitrogen, and phosphorus concentrations were indicative of oligotrophic conditions in all samples despite treated wastewater discharge into the Truckee River by the Truckee Meadows Water Reclamation Facility (TMWRF) 16 km upstream. C:N:P molar ratios were indicative of carbon limitation at IW36 and IW02, nitrogen limitation at RW, and carbon and nitrogen co-limitation at P60, IW25, and IW27 (Redfield 1958). The increase in aggregated concentrations of all dissolved nitrogen species within the MRCB compared to RW and P60, with the exception of IW27, suggests that nitrogen fixation and/or possibly the deamination of proteins serves as an important source of nitrogen for microorganisms inhabiting the MRCB hyporheic zone.

Dissolved oxygen concentrations showed a general declining trend along the longitudinal length of the MRCB (corresponding to the overall downstream longitudinal flow pattern (Shope et al. 2012)) and were much lower in porewater samples (10–36% saturation) compared to RW (102.3% saturation) (Table 1; Figure 2). Consistent with a decline in DO, the concentrations of electron acceptors that might be used under suboxic and anaerobic conditions (NO_3^- and SO_4^{2-}) were also depleted within the channel bar compared to RW and P60, indicative of anaerobic metabolism. Conversely, the concentrations of potential electron donors (Fe^{2+}, Mn^{2+}, and NH_3) were enriched in MRCB porewater compared to RW and P60 (with the exception of IW27), indicative of anaerobic metal reduction (Fe^{2+} and Mn^{2+}), dissimilatory nitrate reduction to NH_3 (Cruz-Garcia et al. 2007; Jetten 2008), and/or anaerobic deamination of proteins during fermentation (Krause and Russell 1996).

Zarnetske et al. (2011) have demonstrated that rates of DO and DOC removal (from heterotrophy) were highest when water residence times were short (<6.9 h) and denitrification rates were highest during longer residence times in a gravel bar hyporheic zone. Despite a sharp decrease in both DO and NO_3^- in the MRCB porewaters, no consistent trend was apparent in the concentrations of DOC, but all were lower in porewaters than in RW (1.7–2.6 mg/L vs. 2.9 mg/L, Table 1; Figure S2). In spite of the slight drop in overall DOC, the pH of porewater within the MRCB was substantially lower than RW and P60 (e.g. 6.65–7.00 vs. 8.18 and 7.6, respectively, Table 1). This result is consistent with the accumulation of organic acid fermentation products being favored over production and accumulation of sulfide from sulfate reduction or loss of CO_2 from autotrophy, especially since DIC increased along the flow path and SO_4^{2-} concentrations were not depleted throughout the MRCB. This is consistent with other studies indicating that an influx of stream water-derived DOC and terminal electron acceptors (e.g. O_2, NO_3^-, SO_4^{2-}) into the hyporheic zone generally stimulates microbial respiration, which results in a decrease in DOC and terminal electron acceptor concentrations and a concomitant increase in DIC (Findlay 1995; Findlay et al. 1993; 2003; Stegen et al. 2018). Furthermore, stimulation of aerobic respiration and metabolism of DOC is particularly pronounced at downwelling zones (Febria et al. 2010; Hendricks 1993; Stegen et al. 2018), which may help explain increased DOC and decreased SO_4^{2-} at IW25 relative to all other porewater samples as this correlates with the location of a significant predicted groundwater mound (upwelling zone).

Despite lower DO concentrations in the hyporheic zone underlying the stream channel (P60) compared to overlying RW, there were no other chemical indications of anaerobic metabolism induction at P60. In aquatic systems, nitrate is generally the first alternative electron acceptor utilized after oxygen (DiChristina 1992; Steinberg et al. 1992; Thauer et al. 1977; Zehnder and Stumm 1988); however, the fact that nitrate concentrations were the same for both RW and P60 suggests that anaerobic metabolism was not strongly induced within the riverbed at this location or that nitrate losses were masked by continual influx of surface water into the subsurface at P60. The latter scenario is not unlikely since this location coincides with the upper boundary of a major riffle structure in a losing reach and the hydraulic conductivity within the streambed was an order of magnitude higher than the MRCB (Shope et al. 2012), indicative of a short water residence time relative to the MRCB. The absence of depletion in sulfate concentrations, which would otherwise be consumed by sulfate-reducing bacteria under anaerobic conditions, also supports overall aerobic conditions within riverbed cobble. Likewise, soluble iron and manganese, which would accumulate due to the activity of anaerobic metal reducers, are not significantly elevated in the riverbed porewater sample. Finally, ammonia, which can result from dissimilatory nitrate reduction (Cruz-Garcia et al. 2007) or from the anaerobic deamination of proteins during fermentation (Krause and Russell 1996), was not

enriched in this sample. Collectively, these data indicate that anaerobic processes within the riverbed are precluded by the presence of oxygen concentrations sufficient to greatly inhibit or prevent anaerobic processes, possibly maintained by infiltration from overlying surface water. However, nitrate reduction and other anaerobic processes may have been occurring at a greater depth than was sampled or in unsampled streambed upwelling zones further downstream.

Whereas indications of complete anoxia were not obtained at any point along the flow path, it is important to note that the short water columns within the piezometers were open to the atmosphere during sampling. Thus, it is likely that actual porewater dissolved oxygen concentrations were lower than detected due to air contamination during pumping/sample collection. Certainly, the removal of nitrate and sulfate and the coincident accumulation of soluble metals (Fe^{2+} and Mn^{2+}) are indicative of the presence of anaerobic microhabitats within the MRCB hyporheic zone. The presence of anaerobic processes within the bulk aerobic hyporheic zone has been reported previously (Hou et al. 2017; Zarnetske et al. 2011). This is generally attributed to stream-derived organic loading causing heterogeneous stimulations in biological oxygen consumption along otherwise oligotrophic and/or oxygenated hyporheic flow paths (Holmes et al. 1996; Morrice et al. 2000). As DOC concentrations in porewater samples were higher throughout the MRCB than at P60, perhaps due to accumulation and degradation of particulate organic matter within the riverbed or within the hyporheic zone (Battin et al. 2008; Stern et al. 2017), it is likely that microbial activity was induced throughout the MRCB. Although this hypothesis was never empirically tested, this possibility is supported by the precipitous decline in dissolved oxygen concentrations between P60 and IW25, an increase in DIC concentrations indicative of carbon metabolism, and observations of stream-derived labile DOC stimulating microbial activity in hyporheic zone fluids of other systems (Findlay 1995; Findlay et al. 1993, 2003; Hendricks 1993).

Although DO concentration was lowest at IW27, only a slight decrease in NO_3^- and SO^{2-} concentrations were observed compared to IW02, directly upstream from IW27 in the MRCB. Additionally, the concentrations of soluble metals and ammonia were much lower (Fe^{2+} was 5× lower, Mn^{2+} was 11× lower, and NH_3 was 19× lower) than IW02. Taken together, these data may be indicative of decreased metabolic productivity, although lateral water flow (southward) from the western river channel to IW27, due to a transient hydraulic gradient observed on 11 September 2007 (Shope et al. 2012) could be responsible for the observed lower concentrations of these dissolved constituents.

Metabolic diversity within the hyporheic zone

Total cell numbers as determined by microscopic direct counts in the porewater samples were consistently lower than those in RW (2.8×10^5–8.1×10^5 vs. 2.5×10^6 cells/mL, Table 2) and were within an order of magnitude of cell counts reported in other hyporheic fluids (Findlay et al. 1993). However, it is unusual to observe higher numbers of cultivable microorganisms than total cell numbers. Typically, cultivable cell counts are lower by several orders of magnitude than direct counts because the majority of environmental microorganisms are considered 'uncultivable' (the so-called great plate count anomaly (Staley and Konopka 1985)). However, this observation must be tempered by the fact that MPN determinations provide approximations of viable cell numbers and that 95% confidence intervals span more than an order of magnitude. Nonetheless, the high concentration of aerobic heterotrophs from the RW sample indicates that the choice of cultivation medium (R2 broth) was appropriate and that a high proportion of the cells in river surface water were capable of growth under aerobic conditions. In the porewater samples, the number of cultivable aerobes as a percentage of total cells decreased precipitously (e.g., cultivable aerobes were 2–3 orders of magnitude lower in abundance than total cells). This result indicates that the microbial populations within the MRCB and in the surface river water were distinct and that many of the cells within the MRCB were adapted to survive under anaerobic/microaerophilic or oligotrophic conditions.

The numbers of cultivable anaerobic microorganisms (as exemplified by sulfate reducers) within the channel bar were highest (5.9×10^3/mL, Table 2) in porewater from IW25 but were detected in all samples, including the fully oxygenated river water. In fact, cultivable iron-reducing microorganisms were only detected in RW. The significance of this result is unclear but could reflect the influence of an upstream wastewater treatment plant, whose discharge represents a significant proportion of stream volume at base flow. It is also possible that, with a longer *in vitro* incubation period or use of a different medium for cultivation, iron reducers would have been detected from the porewater samples.

The greatest loss in nitrate occurred between the riverbed hyporheic zone site (P60) and the most upstream of the channel bar sites (IW36), suggesting that denitrification activity was greatest at the leading edge of the channel bar. In spite of the lack of chemical evidence for denitrification at P60 (Table 1, Figure 2), cultivable denitrifying microorganisms (as verified by MPN, nitrate reduction activity and gas production, Table 2) were most abundant, but overall low in numbers (6.1×10^2 cells/mL), in this sample. The chemical signature of their activity may have been transferred downstream within the riverbed cobble, perhaps reflected in the lower nitrate value we detected and concomitant lower number of cultivable denitrifying microorganisms in porewater from IW36. What may be informative was the very low density of nitrate-reducing microorganisms in sample IW25 (MPN indicating ∼5 cells/mL, Table 2). IW25 loosely corresponds with the location of a significantly predicted groundwater mound (Shope et al. 2012) and thus may be insulated from fresh inputs of river-derived nitrate that would stimulate denitrifying microorganisms. Other than overall lower numbers, no obvious patterns in cultivable denitrifier counts were apparent further along the flow path (IW25, IW02, and IW27). Nitrate concentrations from these sites were uniformly low (0.006–0.003 mg/L), perhaps indicative that denitrification had gone to completion or that

nitrate concentrations were sufficiently low to prevent further nitrate reduction. However, it must be noted that *in situ* metabolic activity was not measured as part of this study.

Prokaryotic diversity within the hyporheic zone

Analyses of prokaryotic community structure through cultivation-independent methods corroborated the cultivation-based metabolic diversity results discussed above. The prokaryotic community of RW was distinct, less diverse, and dominated by unique OTUs compared to all hyporheic zone porewater samples (Tables S2 and S3; Figure 4; Figures S1 and S3). The most abundant OTUs in RW were predicted aerobic heterotrophs, some of which reduce nitrate (e.g., Sporichthyaceae (Tamura et al. 1999) and Comamonadaceae (Willems 2014)). With the exception of the *Acidovorax facilis* OTU, the most dominant OTUs in RW were found in low abundances in all porewater samples (≤0.2% relative abundance each). Given the presence of putative nitrate reducers in the 16S rRNA gene sequence library for RW, and number of cultivable aerobic heterotrophs three orders of magnitude greater than cultivable nitrate reducers (7.0×10^6 cells/mL vs. 5.9×10^3 cells/mL, Table 2) and six orders of magnitude higher than denitrifiers (6.0×10^0 cells/mL), the RW microbial community has the capacity for nitrate reduction, although environmental conditions (in particular, dissolved oxygen concentrations) strongly favored aerobic heterotrophy.

We observed a shift in the predicted metabolic strategy of the abundant OTUs between surface water and porewater: from aerobic heterotrophy to anaerobic, chemolithoautotrophic, and fermentative metabolisms (Table S3). This shift was likely due to suboxic or anaerobic conditions in porewater samples that would have supported these metabolisms (Table 1). River porewater (P60) was dominated by predicted facultative anaerobes, obligate anaerobic fermenters, lithoautotrophs, anoxygenic phototrophs, and aerobic heterotrophs. The dominant OTUs at P60 likely contribute to denitrification and dissolved organic carbon removal. Furthermore, the number of cultivable denitrifiers (as evidenced by nitrate reduction and gas production) from P60 was two orders of magnitude higher than RW (Table 2), likely due to the decreased oxygen concentration in P60, providing additional evidence for a shift in metabolic capacity between the two sites.

The microbial community structure of MRCB porewater samples (IW36, IW02, and IW27) were similar (Figure S2). Dominant OTUs include predicted iron, nitrate, and sulfate reducers, chemolithoautotrophs, and hydrogenotrophic methanogens (Table S3). The high relative abundances of OTUs corresponding with the methanogenic archaeon, *Methanobacterium* spp. in several samples, detected in low relative abundances or completely undetected in RW, P60, and IW25, further suggests strong induction of anaerobic processes within the MRCB. Genera of sulfate-reducing bacteria (*Desulfomicrobium* and *Desulfovibrio*, Table S3) were detected alongside *Methanobacterium* in the MRCB, ranging from 0 to ~1.5% relative abundance. Under high sulfate concentrations, sulfate reducers outcompete methanogens for hydrogen (Kristjansson et al. 1982; Robinson and Tiedje 1984); however, these two groups have been shown to coexist under low sulfate conditions (Stevens and McKinley 1995; Wilms et al. 2007). Further study is needed to elucidate methanogen/sulfate-reducing microbial population dynamics within the MRCB.

It is noteworthy that IW25, despite being comprised of similar taxa as other MRCB communities (Figure S3), prokaryotic organisms detected in IW25 were differentially abundant and the overall abundance-normalized community profile was more similar to P60 and RW (Figure S1). In fact, the most dominant OTUs in IW25 (with the exception of OTU_809, *Hydrogenophaga*) were generally undetected or found in low abundance (<~1.1% relative abundance) in all other samples. As mentioned earlier, IW25 loosely corresponds with the location of a significantly predicted groundwater mound (Shope et al. 2012), which implies that the organisms detected were derived from groundwater. This likely explains why IW25 was dominated by predicted chemolithotrophs (Table S3) found in low abundances in all other samples.

Implications

Hyporheic zones have been classified as 'biogeochemical hotspots' (Craig et al. 2010; McClain et al. 2003; Stegen et al. 2018). In these environments, microorganisms are primarily responsible for up to 75–90% of aerobic respiration (Naegeli and Uehlinger 1997), removal of dissolved nitrate under oxic (Hill and Lymburner 1998; Morrice et al. 2000) and suboxic conditions (Duff and Triska 1990; Holmes et al. 1996; Moser et al. 2003) through nitrate reduction and denitrification, but also contribute to iron, manganese, and sulfur cycling (Moser et al. 2003). Hyporheic zones within partially submerged geomorphic structures have begun to garner attention for their role in DO, DOC, and NO_3^- removal (Zarnetske et al. 2011), and for their higher predicted capacity for denitrification compared to their fully submerged counterparts (Trauth et al. 2015). From our investigation of the microbial ecology of the MRCB, a partially submerged cobble channel bar in the Truckee River, we observed a continuum from oxygenated water dominated by aerobic heterotrophs (RW and, to a lesser extent, P60) to suboxic water dominated by metabolically flexible yet primarily anaerobic microorganisms throughout the MRCB. Both chemical and microbiological evidence suggests that nitrate reduction and denitrification are important processes throughout the MRCB and that partially submerged fluvial environments with sufficient hydraulic gradient and conductivity (Reeder et al. 2018; Zarnetske et al. 2011) are important for nitrate removal and thus improved water quality in rivers. We propose that partially submerged fluvial environments serve as ecologically important zones of enhanced biological activity and that these natural bioreactors possess the capacity for the attenuation of compounds important for water quality and ecosystem health, including nitrate and sulfate.

Acknowledgments

We would like to thank Jim Brock and Chris Fritsen for the use of field instruments, the Nature Conservancy staff at McCarran Ranch for helpful discussions and for providing useful information about the field site, and Mary Miller of the DRI Water Laboratory for chemical analyses. Additionally, we would like to thank two anonymous reviewers for helpful suggestions that improved the manuscript.

Disclosure statement

No potential conflict of interest was reported by the authors.

Funding

This work was supported by the U.S. Army Corps of Engineers Urban Flood Demonstration Program under Cooperative Agreement [W912HZ-08-2-0021].

ORCID

Joshua D. Sackett http://orcid.org/0000-0003-1689-8890

References

Aronesty E. 2011. Ea-Utils: Command-Line Tools for Processing Biological Sequencing Data. Durham, NC: Expression Analysis.

Balch WE, Fox GE, Magrum LJ, Woese CR, Wolfe RS. 1979. Methanogens: reevaluation of a unique biological group. Microbiol Rev. 43(2):260–296.

Battin TJ, Kaplan LA, Findlay S, Hopkinson CS, Marti E, Packman AI, Newbold JD, Sabater F. 2008. Biophysical controls on organic carbon fluxes in fluvial networks. Nature Geosci. 1(2):95.

Caporaso JG, Bittinger K, Bushman FD, DeSantis TZ, Andersen GL, Knight R. 2010. PyNAST: a flexible tool for aligning sequences to a template alignment. Bioinformatics. 26(2):266–267.

Caporaso JG, Kuczynski J, Stombaugh J, Bittinger K, Bushman FD, Costello EK, Fierer N, Pena AG, Goodrich JK, Gordon JI. 2010. QIIME allows analysis of high-throughput community sequencing data. Nat Methods. 7(5):335–336.

Caporaso JG, Lauber CL, Walters WA, Berg-Lyons D, Lozupone CA, Turnbaugh PJ, Fierer N, Knight R. 2011. Global patterns of 16S rRNA diversity at a depth of millions of sequences per sample. Proc Natl Acad Sci Usa. 108(1):4516–4522.

Craig L, Bahr JM, Roden EE. 2010. Localized zones of denitrification in a floodplain aquifer in southern Wisconsin, USA. Hydrogeol J. 18(8):1867–1879.

Cruz-Garcia C, Murray AE, Klappenbach JA, Stewart V, Tiedje JM. 2007. Respiratory nitrate ammonification by *Shewanella oneidensis* MR-1. J Bacteriol. 189(2):656–662.

Dent CL, Grimm NB, Martí E, Edmonds JW, Henry JC, Welter JR. 2007. Variability in surface-subsurface hydrologic interactions and implications for nutrient retention in an arid-land stream. J Geophys Res: Biogeosci. 112(G4):1–13.

DiChristina TJ. 1992. Effects of nitrate and nitrite on dissimilatory iron reduction by *Shewanella putrefaciens* 200. J Bacteriol. 174(6): 1891–1896.

Duff JH, Triska FJ. 1990. Denitrification in sediments from the hyporheic zone adjacent to a small forested stream. Can J Fish Aquat Sci. 46:2240–2247.

Edgar RC. 2010. Search and clustering orders of magnitude faster than BLAST. Bioinformatics. 26(19):2460–2461.

Febria CM, Fulthorpe RR, Williams DD. 2010. Characterizing seasonal changes in physicochemistry and bacterial community composition in hyporheic sediments. Hydrobiologia. 647(1):113–126.

Findlay S. 1995. Importance of surface-subsurface exchange in stream ecosystems: the hyporheic zone. Limnol Oceanogr. 40(1):159–164.

Findlay S, Strayer D, Goumbala C, Gould K. 1993. Metabolism of streamwater dissolved organic-carbon in the shallow hyporheic zone. Limnol Oceanogr. 38(7):1493–1499.

Findlay SEG, Sinsabaugh RL, Sobczak WV, Hoostal M. 2003. Metabolic and structural response of hyporheic microbial communities to variations in supply of dissolved organic matter. Limnol Oceanogr. 48(4):1608–1617.

Francis BA, Francis LK, Cardenas MB. 2010. Water table dynamics and groundwater-surface water interaction during filling and draining of a large fluvial island due to dam-induced river stage fluctuations. Water Resour Res. 46(7):7513.

Goldman AE, Graham EB, Crump AR, Kennedy DW, Romero EB, Anderson CG, Dana KL, Resch CT, Fredrickson JK, Stegen JC. 2017. Biogeochemical cycling at the aquatic–terrestrial interface is linked to parafluvial hyporheic zone inundation history. Biogeosciences. 14(18):4229–4241.

Greenberg AE, Clesceri LS, Eaton AD, editors. 1992. Standard Methods for the Examination of Water and Wastewater. 18th ed. Section 9–15. Washington, DC: American Public Health Association.

Hendricks SP. 1993. Microbial ecology of the hyporheic zone - a perspective integrating hydrology and biology. J N Am Benthol Soc. 12(1):70–78.

Hill AR, Lymburner DJ. 1998. Hyporheic zone chemistry and stream-subsurface exchange in two groundwater-fed streams. Can J Fish Aquat Sci. 55(2):495–506.

Holmes RM, Jones JB, Fisher SG, Grimm NB. 1996. Denitrification in a nitrogen-limited stream ecosystem. Biogeochemistry. 33(2):125–146.

Hou Z, Nelson WC, Stegen JC, Murray CJ, Arntzen E, Crump AR, Kennedy DW, Perkins MC, Scheibe TD, Fredrickson JK, et al. 2017. Geochemical and microbial community attributes in relation to hyporheic zone geological facies. Sci Rep. 7(1):12006.

Jetten MS. 2008. The microbial nitrogen cycle. Environ Microbiol. 10(11):2903–2909.

Kostka JE, Nealson KH. 1998. Isolation, cultivation, and characterization of iron- and manganese-reducing bacteria. In: Burlage RS, Atlas R, Stahl D, Sayler G, editors. Techniques in Microbial Ecology. New York, NY: Oxford University Press, p468.

Krause DO, Russell JB. 1996. An rRNA approach for assessing the role of obligate amino acid-fermenting bacteria in ruminal amino acid deamination. Appl Environ Microbiol. 62(3):815–821.

Kristjansson JK, Schönheit P, Thauer RK. 1982. Different K_s values for hydrogen of methanogenic bacteria and sulfate reducing bacteria - an explanation for the apparent inhibition of methanogenesis by sulfate. Arch Microbiol. 131(3):278–282.

Lefebvre S, Marmonier P, Pinay G. 2004. Stream regulation and nitrogen dynamics in sediment interstices: comparison of natural and straightened sectors of a third-order stream. River Res Applic. 20(5):499–512.

Lozupone C, Lladser ME, Knights D, Stombaugh J, Knight R. 2011. UniFrac: an effective distance metric for microbial community comparison. Isme J. 5(2):169–172.

McClain ME, Boyer EW, Dent CL, Gergel SE, Grimm NB, Groffman PM, Hart SC, Harvey JW, Johnston CA, Mayorga E, et al. 2003. Biogeochemical hot spots and hot moments at the interface of terrestrial and aquatic ecosystems. Ecosystems. 6(4):301–312.

Miller TL, Wolin MJ. 1974. A serum bottle modification of the Hungate technique for cultivating obligate anaerobes. Appl Microbiol. 27(5):985–987.

Morrice JA, Dahm CN, Valett M, Unnikrishna PV, Campana ME. 2000. Terminal electron accepting processes in the alluvial sediments of a headwater stream. J N Am Benthol Soc. 19(4):593–608.

Mortensen ER, Cath TY, Brant JA, Dennett KE, Childress AE. 2007. Evaluation of membrane processes for reducing total dissolved solids discharged to the Truckee river. J Environ Eng. 133(12):1136–1144.

Moser DP, Fredrickson JK, Geist DR, Arntzen EV, Peacock AD, Li SMW, Spadoni T, McKinley JP. 2003. Biogeochemical processes and microbial characteristics across groundwater-surface water boundaries of the Hanford Reach of the Columbia River. Environ Sci Technol. 37(22):5127–5134.

Moser DP, Nealson KH. 1996. Growth of the facultative anaerobe *Shewanella putrefaciens* by elemental sulfur reduction. Appl Environ Microbiol. 62(6):2100–2105.

Myers CR, Nealson KH. 1988. Bacterial manganese reduction and growth with manganese oxide as the sole electron acceptor. Science. 240(4857):1319–1321.

Naegeli MW, Uehlinger U. 1997. Contribution of the hyporheic zone to ecosystem metabolism in a prealpine gravel-bed river. J N Am Benthol Soc. 16(4):794–804.

Ock G, Gaeuman D, McSloy J, Kondolf GM. 2015. Ecological functions of restored gravel bars, the Trinity River, California. Ecol Eng. 83: 49–60.

Oksanen J, Blanchet FG, Kindt R, Legendre P, O'Hara RB, Simpson GL, Solymos P, Stevens MHH, Wagner H. 2015. Vegan: Community Ecology Package. Accessed February 17, 2018. Available at https://cran.r-project.org/web/packages/vegan/index.html

Osterkamp WR. 1998. Processes of fluvial island formation, with examples from Plum Creek, Colorado and Snake River, Idaho. Wetlands. 18(4):530–545.

Parada AE, Needham DM, Fuhrman JA. 2016. Every base matters: assessing small subunit rRNA primers for marine microbiomes with mock communities, time series and global field samples. Environ Microbiol. 18(5):1403–1414.

Paradis E, Claude J, Strimmer K. 2004. APE: analyses of phylogenetics and evolution in R language. Bioinformatics. 20(2):289–290.

Porter K, Feig YS. 1980. The use of DAPI for identifying and counting the aquatic microflora. Limnol Oceanogr. 25(5):943–948.

Postgate JR. 1984. The Sulphate-Reducing Bacteria, 2nd ed. Cambridge, UK: Cambridge University Press.

Price MN, Dehal PS, Arkin AP. 2010. FastTree 2-approximately maximum-likelihood trees for large alignments. Plos One. 5(3):e9490.

Pruesse E, Quast C, Knittel K, Fuchs BM, Ludwig WG, Peplies J, Glockner FO. 2007. SILVA: a comprehensive online resource for quality checked and aligned ribosomal RNA sequence data compatible with ARB. Nucleic Acids Res. 35(21):7188–7196.

Quast C, Pruesse E, Yilmaz P, Gerken J, Schweer T, Yarza P, Peplies J, Glockner FO. 2013. The SILVA ribosomal RNA gene database project: improved data processing and web-based tools. Nucleic Acids Res. 41(D1):D590–D596.

R Core Team. 2014. R: A Language and Environment for Statistical Computing. Vienna, Austria.

Reasoner DJ, Geldreich EE. 1985. A new medium for the enumeration and subculture of bacteria from potable water. Appl Environ Microbiol. 49(1):1–7.

Redfield AC. 1958. The biological control of chemical factors in the environment. Am Sci. 46(3):205–221.

Reeder WJ, Quick AM, Farrell TB, Benner SG, Feris KP, Tonina D. 2018. Spatial and temporal dynamics of dissolved oxygen concentrations and bioactivity in the hyporheic zone. Water Resour Res. 54(3):2112–2128.

Robinson JA, Tiedje JM. 1984. Competition between sulfate-reducing and methanogenic bacteria for H2 under resting and growing conditions. Arch Microbiol. 137(1):26–32.

Schmidt C, Musolff A, Trauth N, Vieweg M, Fleckenstein JH. 2012. Transient analysis of fluctuations of electrical conductivity as tracer in the stream bed. Hydrol Earth Syst Sci. 16(10):3689–3697.

Shope CL, Constantz JE, Cooper CA, Reeves DM, Pohll G, McKay WA. 2012. Influence of a large fluvial island, streambed, and stream bank on surface water-groundwater fluxes and water table dynamics. Water Resour Res. 48(6):W06512.

Staley JT, Konopka A. 1985. Measurement of in situ activities of nonphotosynthetic microorganisms in aquatic and terrestrial habitats. Annu Rev Microbiol. 39(1):321–346.

Stegen JC, Johnson T, Fredrickson JK, Wilkins MJ, Konopka AE, Nelson WC, Arntzen EV, Chrisler WB, Chu RK, Fansler SJ, et al. 2018. Influences of organic carbon speciation on hyporheic corridor biogeochemistry and microbial ecology. Nat Commun. 9(1):585.

Steinberg NA, Blum JS, Hochstein L, Oremland RS. 1992. Nitrate is a preferred electron acceptor for growth of freshwater selenate-respiring bacteria. Appl Environ Microbiol. 58(1):426–428.

Stern N, Ginder-Vogel M, Stegen JC, Arntzen E, Kennedy DW, Larget BR, Roden EE. 2017. Colonization habitat controls biomass, composition, and metabolic activity of attached microbial communities in the Columbia River hyporheic corridor. Appl Environ Microbiol. 83(16):e00260.

Stevens TO, McKinley JP. 1995. Lithoautotrophic microbial ecosystems in deep basalt aquifers. Science. 270(5235):450–454.

Tamura T, Hayakawa M, Hatano K. 1999. *Sporichthya brevicatena* sp nov. Int J Syst Bacteriol. 49(4):1779–1784.

Thauer RK, Jungermann K, Decker K. 1977. Energy conservation in chemotrophic anaerobic bacteria. Bacteriol Rev. 41(1):100–180.

Trauth N, Schmidt C, Vieweg M, Oswald SE, Fleckenstein JH. 2015. Hydraulic controls of in-stream gravel bar hyporheic exchange and reactions. Water Resour Res. 51(4):2243–2263.

USEPA. 1979. Methods for Chemical Analysis of Water and Wastes. Vol. EPA-600/4-79-020. Cincinnati, OH: USEPA.

USEPA. 1993. Methods for the Determination of Inorganic Substances in Environmental Samples. Vol. EPA/600/R-93/100. Washington, DC: USEPA.

USGS. 2017. U.S. Geological Survey. National Water Information System data available on the World Wide Web (USGS Water Data for the Nation). Accessed February 5, 2019. Available at https://waterdata.usgs.gov/nwis/.

Willems A, et al. 2014. The family Comamonadaceae. In: Rosenberg E, DeLong EF, Lory S., editors. The Prokaryotes: Alphaproteobacteria and Betaproteobacteria. Berlin, Heidelberg: Springer, p777–851.

Wilms R, Sass H, Kopke B, Cypionka H, Engelen B. 2007. Methane and sulfate profiles within the subsurface of a tidal flat are reflected by the distribution of sulfate-reducing bacteria and methanogenic archaea. FEMS Microbiol Ecol. 59(3):611–621.

Woomer PL. 1994. Most probable number counts. In: Bigham JM, and S.H. Mickelson, editors. Methods of Soil Analysis, Part 2 Microbiological and Biochemical Properties-SSSSA Book Series. Madison, WI: Soil Science Society of America, p59–79.

Yilmaz P, Parfrey LW, Yarza P, Gerken J, Pruesse E, Quast C, Schweer T, Peplies J, Ludwig W, Glockner FO. 2014. The SILVA and "All-species Living Tree Project (LTP)" taxonomic frameworks. Nucl Acids Res. 42(D1):D643–D648.

Zarnetske JP, Haggerty R, Wondzell SM, Baker MA. 2011. Dynamics of nitrate production and removal as a function of residence time in the hyporheic zone. J Geophys Res. 116(G1):1–12.

Zehnder AJB, Stumm W. 1988. Geochemistry and biogeochemistry of anaerobic habitats. In: Zehnder AJB, editor. Biology of Anaerobic Microorganisms. New York, NY: John Wiley and Sons, p1–38.